Supplementary Materials for

In vivo microscopy reveals a tumor-associated macrophage mediated resistance pathway in anti-PD-1 therapy

Sean P. Arlauckas*, Christopher S. Garris*, Rainer H. Kohler, Maya Kitaoka, Michael F. Cuccarese, Katherine S. Yang, Miles A. Miller, Jonathan C. Carlson, Gordon J. Freeman, Robert M. Anthony, Ralph Weissleder, Mikael J. Pittet #

*Contributed equally
#Corresponding author. E-mail: mpittet@mgh.harvard.edu

This document includes:

Supplementary Methods

Materials

Rat IgG2a kappa anti-mouse PD1 29F.1A12 clone was kindly provided by Gordon Freeman (DFCI). The SAIVI Alexa Fluor 647 Antibody/Protein 1 mg-Labeling Kit (ThermoFisher Scientific) was used to label Rat IgG2a isotype control clone 2A3 (BioXcell, Lebanon, NH), rat anti-mouse PD-1 IgG2a clone 29F.1A12, the deglycosylated rat anti-mouse PD-1 IgG2a, and nivolumab (Bristol-Myers Squibb, New York, NY) with a covalently-attached and photo-stable Alexa Fluor 647. Dextran nanoparticles preferentially accumulate in macrophages and are commonly used as an *in vivo* macrophage imaging agent (*23*). Ferumoxytol (60 mg Fe, AMAG Pharmaceuticals, Waltham, MA) was dialyzed overnight against water, aminated overnight at r.t. in a 6.5 mL solution containing 1 g (N-3-dimethylaminopropyl)-N-ethylcarbodiimide hydrochloride and 0.6 nM ethylenediamine dihydrochloride, and dialyzed at pH 8 in a 0.02 M Na-citrate buffer containing 0.15 M NaCl. Pacific Blue-succinimidyl ester (5 mg, Thermo Fisher Scientific, Waltham, MA) was dissolved in DMF and 0.6 mL was incubated overnight with 2 mL aminated dextran nanoparticle at r.t. Free dye was removed using PD-10 columns (GE Healthcare, Little Chalfont, UK). Pacific Blue-SE (Life Technologies) was also used to label 500 kDa amino-dextran (Thermo Fisher Scientific) according to the manufacturer's instructions. The 29F.1A12 rat anti-mouse PD1, nivolumab, and human IVIG (a kind gift from Harry Meade, LFB USA) were natively deglycosylated in parallel using PNGase F (New England Biolabs) following manufacturers' protocols. The de-glycosylated antibodies were purified using Protein G beads (Pierce Biotechnology, Waltham,

MA). Antibody glycan profiling was performed as previously described (*45*), using an Agilent HPLC 1260, with Agilent AdvanceBio Glycan Mapping HILIC-based column. Glycoforms were identified by referencing the elution times of the digested glycans from the IVIG standard. Rat anti-mouse CD16/32 clone 2.4G2 (BioXcell) was used for *in vivo* FcγR blocking (*46*).

Cell models

Cell lines were maintained in Iscove's growth medium supplemented with 10% heat inactivated Fetal Calf Serum (Atlanta Biologicals) and 100 IU penicillin, 100 µg/ml streptomycin (Invitrogen) at 37°C and 5% CO_2 and checked monthly for mycoplasma. The MC38 mouse colon adenocarcinoma cell lines were kindly provided by Mark Smyth (QIMR Berghofer Medical Research Institute). MC38 cells were transfected with an H2B-mApple reporter for imaging as previously described (47). Briefly, cells were cultured in a 24-well dish and transfected with the pLVX-H2B-mApple lentiviral vector (Clonetech) in the presence of 10 µg/mL polybrene (Santa Cruz Biotech). Fresh media was provided after 24 hours, and cells were split the following day into 3 µg/mL puromycin for selection. A homogenous population of transfected MC38-H2B-mApple was obtained by FACS sorting. The murine lymphoma EL4 cell line was acquired from ATCC. Suspended cells were passed before they reached densities exceeding 1 x 10^6 cells/mL. Murine bone marrow-derived macrophages (BMDMs) were isolated from surgically-resected femurs and tibias of C57BL/6J mice. Under sterile conditions, bone marrow was flushed from the bone using a PBS-filled syringe and a 28-gauge needle. Cells were spun down and red blood cells lysed with ammonium chloride at 4°C for 5 minutes. The remaining cells were plated in growth medium supplemented with 10 ng/mL of murine macrophage-colony stimulating factor (M-CSF, Peprotech, Rocky Hill, NJ). M-CSF supplemented media was replaced every 2 days. Human peripheral blood mononuclear cells (PBMCs) from healthy donors were carefully isolated from buffy coats spun down on a Ficoll-Paque PLUS gradient (GE Life Sciences) using the manufacturer's protocol. These cells were plated in petri plates and maintained in 50 ng/mL of human M-CSF (Peprotech) with media changes every 3 days. $CD8^+$ lymphocytes were also isolated from donor-matched PBMCs using the Human $CD8^+$ T Cell Isolation Kit (Miltenyi Biotec, Auburn, CA). $CD8^+$ lymphocytes were cultured on 24-well plates that were pre-coated overnight with an anti-CD3 antibody clone OKT3 (BD Biosciences) to induce PD-1 expression. Cells were stimulated for 3 days before use in bioassays.

Fluorescence reflectance imaging

Gross examination of AF647-aPD-1 bio-distribution was performed in an Olympus OV100 imaging system. C57BL/6J mice were shaved and inoculated intradermally on the flank with 2 x 10^6 MC38 tumor cells in 50 µL PBS. When tumors reached approximately 30 mm^2 (8 days), mice were assigned to treatment cohorts and given one injection of 200 µg AF647-aPD-1 intravenously. A vehicle control group received unlabeled rat IgG2a isotype control. Mice were sacrificed 30 minutes, 4 hours, 24 hours, or 72 hours post-treatment and tissues of interest were surgically resected, rinsed with saline, and imaged using an Olympus OV100 with brightfield acquisition (122 ms exposure time) or corresponding fluorescence filters (1000 ms exposure time). Mean fluorescence intensity values from ROIs manually drawn around each organ in ImageJ were background-corrected and reported as a ratio relative to the control-treated cohort.

Flow cytometry

Spleen and lymph nodes were minced and passed through 40 micron filters (BD Falcon), whereas lung and tumor tissue were first digested in RPMI containing 0.2 mg/ml collagenase II (Worthington) at 37°C for 30 minutes and then passed through a 40 micron filter. Red blood cells were lysed using ACK lysis buffer (Thermo Fisher Scientific). Cells were pre-treated with FcγR block (TruStain FcX anti CD16/32 clone 93, BioLegend, San Diego, CA) before staining with fluorochrome labeled antibodies, CD90.2 (53-2.1, BD), CD11b (M1/70, Biolegend), CD8a (53-6.7, BD), CD45 (30-F11, BD), F4/80 (BM8, Biolegend), CD11c (N418, Biolegend), CD4 (RM4-5, BD), NK1.1 (PK136, BD), B220 (RA3-6B2, BD), in buffer containing 0.5% BSA and 2 mM EDTA. 7AAD was used to exclude dead cells from analysis. EL4 cells were used as a positive control for aPD-1 staining in our analyses. For antibody shaving/ internalization studies, surface aPD-1 was removed using an acid wash (RPMI 1640, 2% FCS, pH 2) method previously described (48). Re-probing the T cells with PE-aPD-1 (RMP1-14, Biolegend) was used to quantitate remaining surface expression of PD-1 protein. Rat anti-mouse PD-1 was also detected in tumor tissue using anti-rat IgG2a (R2A-21B2, eBiosciences) with the following fluorochrome-labeled rat anti-mouse IgG2b antibodies: CD8b (YTS156.7.8, Biolegend), MHCII (M5/114.15.2, eBioscience), CD45 (30-F11, eBioscience), CD11b (M1/70, BD), and Hamster anti-

mouse CD11c (N418, Biolegend). To block FcγRs, these cells were pre-treated with rat IgG2b anti-mouse CD16/CD32 (2.4G2, Tonbo) and purified mouse IgG1 anti-mouse CD64 (X54-5/7.1, Biolegend). Cells were fixed and permeabilized using CytoFix CytoPerm (BD) for intracellular staining. Samples were run on a LSR II flow cytometer (BD) and analyzed using FlowJo software (Treestar).

Intravital imaging

Mice were anesthetized and hair on the flank removed by shaving and 30 seconds of NAIR application. Dorsal skin-fold window chambers were installed as previously described (*44, 49*) and mice were kept on analgesic for the next 72 hours. One day after window placement, the top skin layer was removed using sterile instruments. At least 24 hours was allowed for resolution of swelling in the window chamber, then MC38-H2B-mApple cells (2×10^6 in 20 µL) were injected in the fascia layer. Tumor growth was carefully monitored for the next 7 days. Time-lapse imaging was performed 8 days after inoculation. Pacific Blue-dextran nanoparticle (containing 1 nmol Pacific Blue dye) was injected i.v. 24 hours prior to imaging for macrophage labeling. A 30-gauge catheter was placed in the tail vein of an anesthetized mouse (2% isoflurane in oxygen) and Pacific Blue-dextran (containing 37 µg dextran and 56 nmol Pacific Blue dye) was injected for vascular labeling. Mice were maintained under anesthesia on a heating pad kept at 37°C and imaged using an Olympus FluoView FV1000MPE confocal imaging system (Olympus America). Vascularized regions were selected using a 2x air objective XL Fluor 2x/340 (NA 0.14; Olympus America), before switching to a XLUMPLFL 20× water immersion objective (NA 0.95; Olympus America) for high resolution imaging with 2x digital zoom. Z-stack acquisition settings (e.g. voltage and laser power) were optimized for sequential scanning of 5 µm slices using 405, 473, 559, and 635 nm lasers paired with a DM405/473/559/635 nm dichroic beam splitter. The beam splitters (SDM473, SDM560, and SDM 640) and emission filters (BA430-455, BA490-540, BA575-620, BA575-675) required for acquisition of emitted light were sourced from Olympus America. For pharmacokinetic analysis, a time-course using 8 ms scan speed for a total frame interval of 183 seconds was acquired at two non-overlapping coordinates, during which the AF647-aPD-1 mAb was delivered via catheter. Cell motility measurements were made 20 minutes before and 20 minutes after AF647-aPD-1 injection using time lapse images acquired with higher temporal resolution (frame interval of 21 seconds). The Manual Tracking Plugin included in the FIJI image processing package was used

to characterize cell tracks. Cell motility coefficients (M) were calculated from each cell track using the slope of the regression function fitted to the mean displacement plot, according to the following formula: $M = d^2 / 4t$, where d is displacement from origin at time t (50). Track plots were creating using the Chemotaxis and Migration Tool for ImageJ (IBIDI).

Live cell imaging

BMDMs cultured for 6 days in 35 mm poly-D-lysine coated 14 mm glass-bottom 35 mm dishes (Mattek, Ashland, MA) were stained with the PKH26-Red staining kit (Sigma-Aldrich) following the manufacturer's protocol. PD-1 expressing EL-4 T cells were stained with the PKH67-Green Fluorescent Cell Linker kit (Sigma-Aldrich), then stained with either AF647-rat IgG2a isotype control (InVivoMAb), AF647-aPD-1 mAb, or de-glycosylated AF647-aPD-1 mAb as indicated. After thorough washing, labeled T cells were added in co-culture to the BMDM dishes placed within the 8 carousel positions of a VivaView FL incubator fluorescence inverted microscope (LCV110, Olympus America). Images were acquired in each sample every 5 minutes using a 20x objective with 0.5x zoom, and live cell tracking was performed in the presence of vehicle control, Fc block (TruStain FcX), anti-FcγRIV 9e9 antibody (generously provided by Robert Anthony) (*51*), or Dynasore (80 μM, Sigma-Aldrich). Human PBMC/ $CD8^+$ T-cell co-cultures were stained using the same PKH26-Red and PKH67-Green kit protocols described for murine BMDM : T cell cultures, and AF647-nivolumab was used to stain anti-CD3 stimulated $CD8^+$ lymphocytes. Human Fc receptor block (TruStain FcX, BioLegend) was used where indicated.

Image Processing

Image files were prepared for figure panels using the FIJI package of ImageJ for pseudo-coloring fluorescent channels, adjusting background/contrast, and creating Z-projections. For *in vivo* object segmentation, rolling ball background subtraction and thresholding using the Otsu method were used to create object masks for cells and vessels. AF647-aPD-1 intensity levels were measured within ROIs created from the indicated object masks. At low concentrations, fluorescence intensity approaches linearity with concentration, and the fluorescence intensity ratio at time (I_t) and pre-injection (I_0) was used to report C_t / C_0. *In vitro* image analysis, including $PD\text{-}1^+$ puncta quantification, was performed

using a custom CellProfiler pipeline. Macrophages were segmented using the Otsu threshold method and macrophages that did not come in contact with lymphocytes were excluded. The speckle counting function in CellProfiler was used to quantitate puncta.

Rat IgG2a detection assay

EL-4 T cells were labeled with AF647-aPD-1 and co-cultured for 2 hours with mouse bone marrow derived macrophages (BMDM). The supernatant containing non-adherent T cells was removed and the BMDM monolayer was washed 3x with PBS. Flow cytometric analysis was used to confirm removal of T cells. Fresh media was then added to the BMDM monolayers and cells were incubated for 0 or 4 hours before being scraped, collected into microcentrifuge tubes, and frozen overnight. Samples were concentrated using Amicon Ultra-0.5 mL Centrifugal Filters with a 30 kDa cut-off (Millipore), and the rat IgG2a content measured using the Rat IgG ELISA kit (eBioscience) following the manufacturers instructions and a Tecan Safire 2 fluorescence plate reader. Parallel co-culture experiments were performed, but the cells were scraped in MACS buffer, stained with F4/80 and CD90 antibodies to distinguish BMDM from T cells, and the AF647 binding tropism was independently measured at the indicated time points.

Supplementary Figures

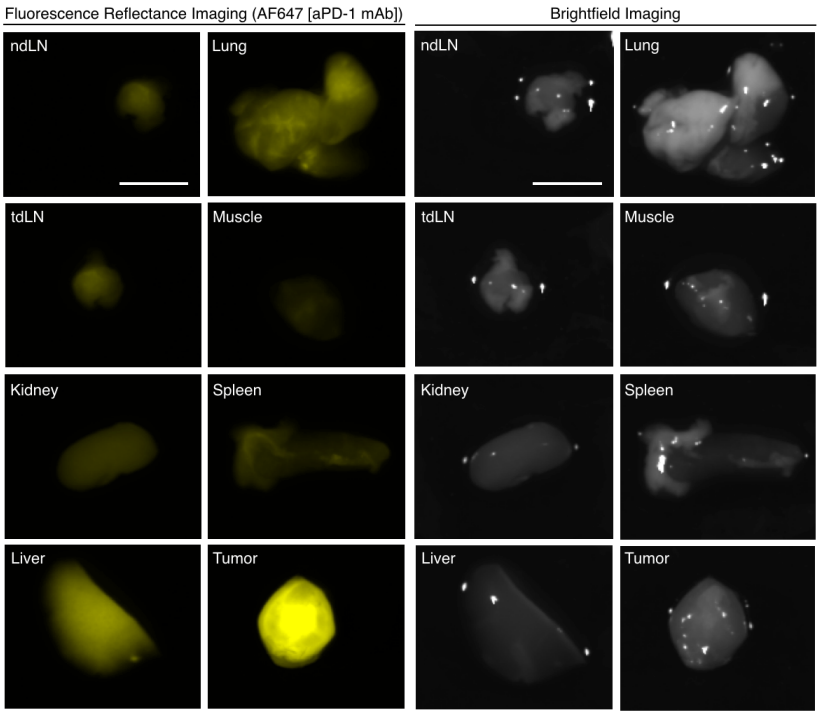

Figure S1: AF647-aPD-1 mAb quantification in various tissues at 24 h post injection.

Fluorescence reflectance imaging (left) was used to detect AF647-aPD-1 mAb within various tissues, which were resected from MC38 tumor-bearing mice at 24 h post drug administration (AF647: λ_{ex} = 620–650 nm, λ_{em} = 680–710 nm). Bright-field images of the same field of views are also shown (right). Scale bar represents 5 mm. ndLN: non-draining lymph node; dLN: tumor-draining LN.

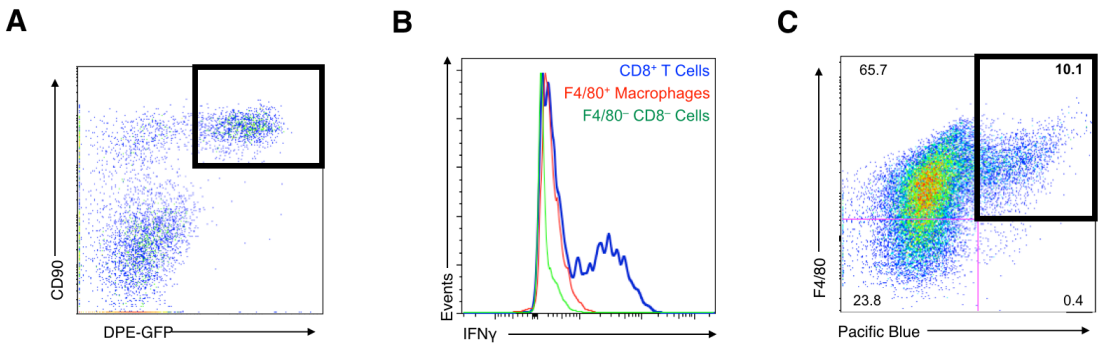

Figure S2: Specificity of T cell reporter mice and dextran nanoparticle. (A) Representative flow cytometry plot of tumor-infiltrating cells obtained from a MC38 tumor-bearing DPE-GFP mouse, indicating that DPE-GFP$^+$ cells are also CD90$^+$ (T cell marker). **(B)** IFNγ reporter expression profiles of various tumor-infiltrating immune cell populations obtained from a MC38 tumor-bearing IFNγ reporter (GREAT) mouse. Cell populations shown are: CD8$^+$ T cells (blue, pre-gated as CD3$^+$ CD8$^+$), macrophages (red, pre-gated as F4/80$^+$), and remaining F4/80$^-$ CD8$^-$ cells (green). **(C)** Representative flow cytometry dot plot of MC38 tumor-bearing mice injected 24 hours prior with Pacific Blue-dextran nanoparticle shows uptake specific to F4/80$^+$ cells pre-gated for CD45.

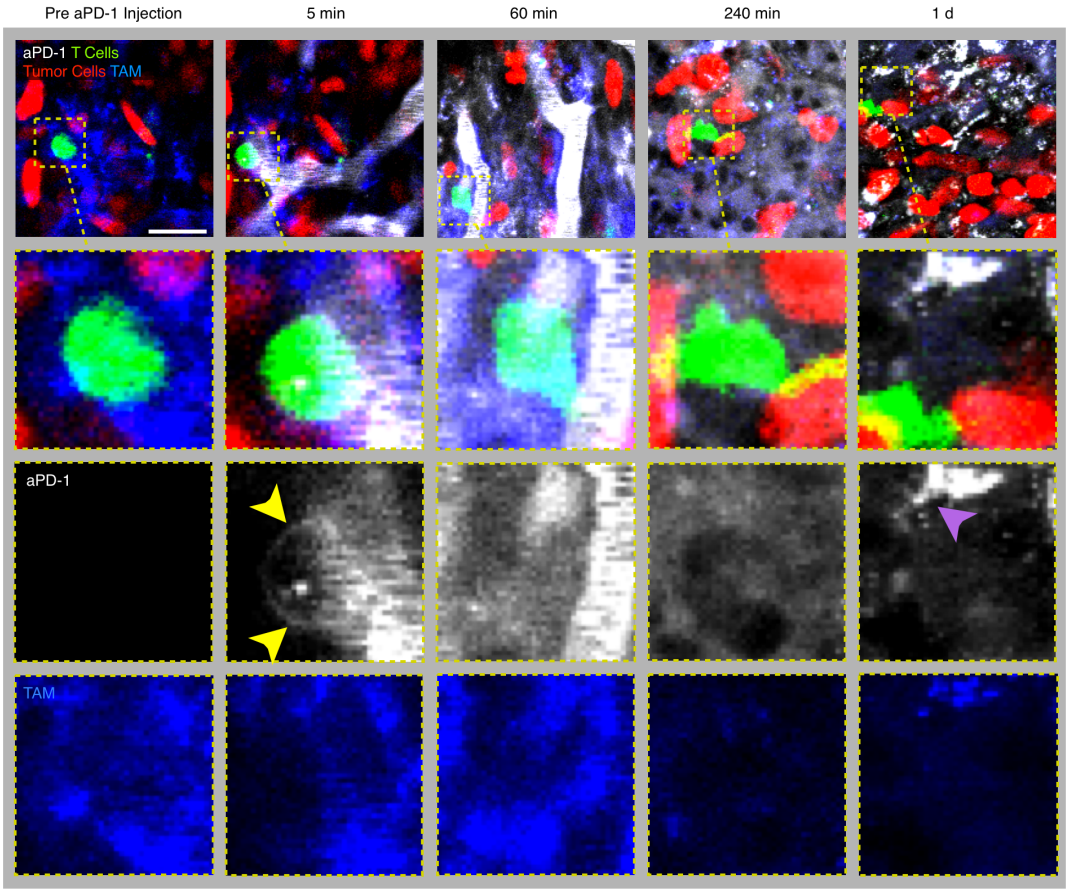

Figure S3: **Representative intravital microscopy time-course of AF647-aPD-1 from an IFNγ-YFP mouse.** Intravital imaging time-lapses are depicted from the the dorsal skin fold chamber of a MC38-H2B-mApple tumor bearing GREAT mouse injected with a macrophage-targeted Pacific Blue-dextran nanoparticle. Injection with AF647-aPD-1 at time zero permitted tracking of drug distribution in multiple cells and compartments. Yellow boxes represent regions shown at higher zoom. At 5 minutes, pericellular staining of AF647-aPD-1 on an IFNγ expressing $CD8^+$ T cell in close proximity to a blood vessel is observed (identified with yellow arrows). AF647-aPD1 is mainly interstitial in 60 and 240 minute images, and collected in macrophages (purple arrow) after 1 day. Yellow regions at the green/red interface after 240 minutes represent interactions between $CD8^+$ T cells and tumor cells. These images are projections of Z-stacks with 5 μm thickness. Scale bars represent 30 μm.

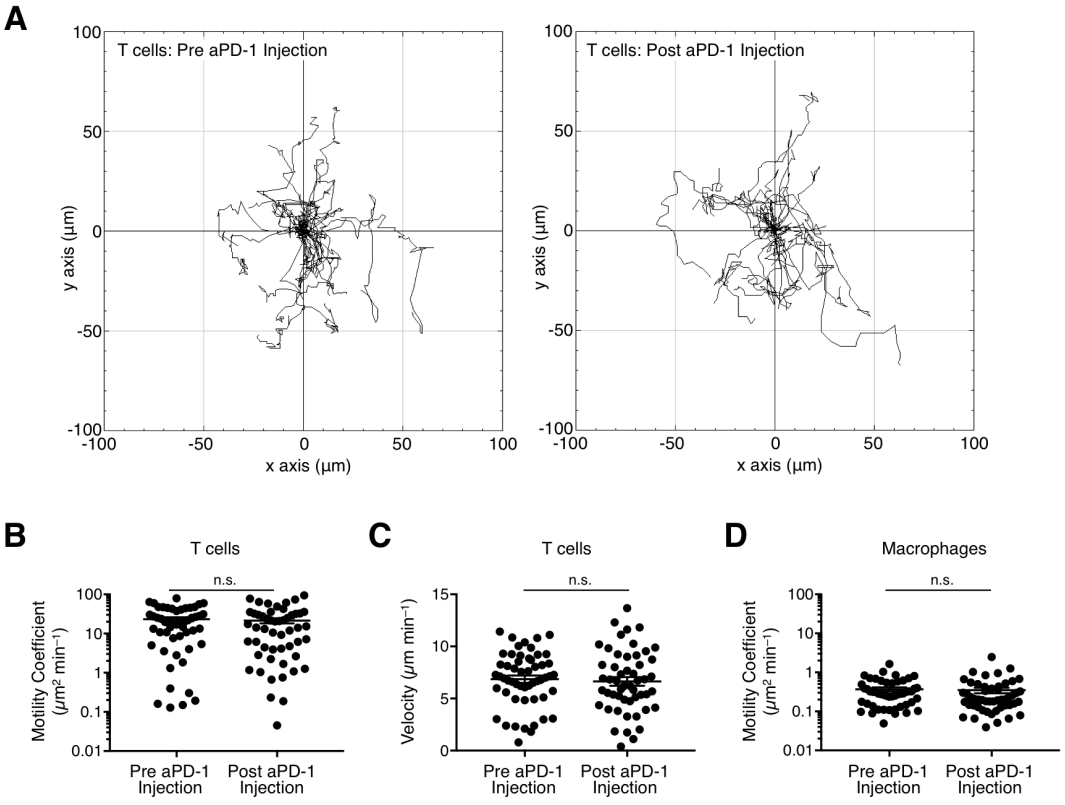

Figure S4: T cell and macrophage motility before and after aPD-1 treatment. (A) Track plots of GREAT mouse T cells imaged using intravital microscopy. **(B)** Motility coefficients of individual T cell tracks were not significantly different after aPD-1 injection. **(C)** Instantaneous T cell velocity did not change after treatment. **(D)** Tumor macrophage motility coefficients showed the cells to be stationary before and after aPD-1 injection. Pre-treatment refers to a 20 minute period before aPD-1 injection, and post-treatment refers to a 20 minute period after aPD-1 injection.

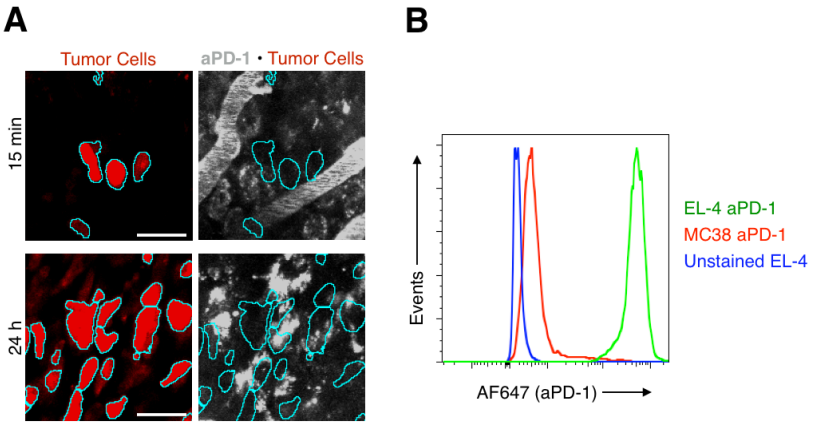

Figure S5: aPD-1 does not directly bind tumor cells. (A) *In vivo* microscopy in the dorsal skin fold chamber of a GREAT mouse with MC38/H2B-mApple tumor cells (cerulean outline) revealed no evidence of AF647-aPD-1 binding to tumor cells at any of the times investigated; scale bars represent 30 µm. **(B)** Lack of AF647-aPD-1 binding to tumor cells is consistent with flow cytometry histograms demonstrating no PD-1 expression in MC38 tumor cells. Stained and unstained EL4 cells were used as positive and negative control samples.

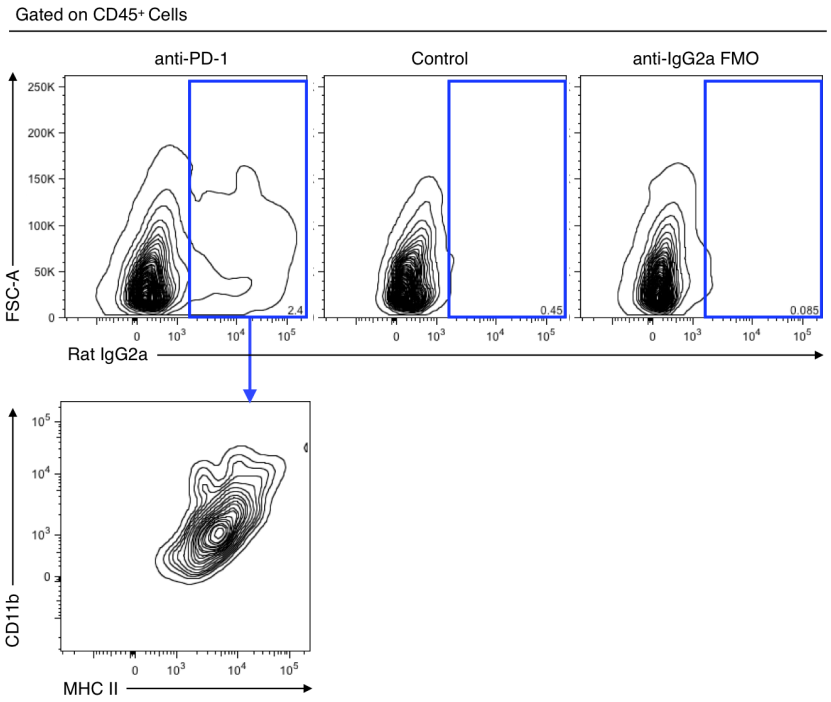

Figure S6: Anti-Rat IgG2a staining to detect aPD-1 transferred *in vivo* to macrophages. Mice bearing MC38 tumors were sacrificed 2 h after receiving aPD-1. Single cell suspensions from tumors were fixed, permeabilized, and stained for multicolor flow cytometry to identify aPD-1 (Rat IgG2a) in tumor macrophages ($CD45^+$ $CD11b^+$ $MHCII^+$), confirming that the antibody is shaved *in vivo*

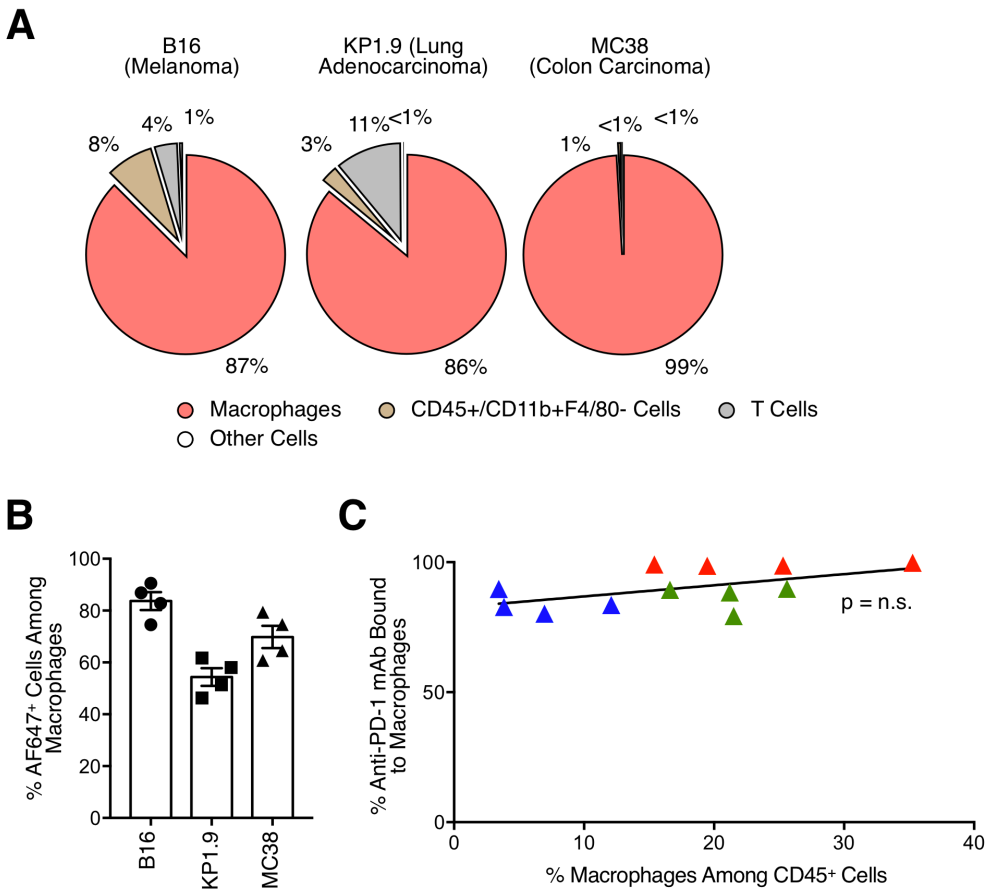

Figure S7: Distribution of AF647-aPD-1 across tumor models. Mice bearing the indicated tumors were sacrificed 24 h after receiving AF647-aPD-1. **(A)** Multicolor flow cytometry was performed *ex vivo* to identify AF647-aPD-1 cellular distribution among immune cell types, including macrophages ($CD45^+$ $7AAD^-$ $F4/80^+$ $CD11c^+$), T cells ($CD45^+$ $7AAD^-$ $CD90^+$ $CD11b^-$), $CD45^+$ $7AAD^-$ $CD11b^+$ $F4/80^-$ cells that include granulocytes/monocytes, and other immune cells ($CD45^+$ $7AAD^-$ $CD90^-$ $CD11b^-$ $F4/80^-$ $CD11c^-$) Data are averages of 4 independent samples. **(B)** Percentage of tumor-associated macrophages accumulating AF647-aPD-1. n = 4 for each tumor type. **(C)** AF647-aPD-1 binding ability to tumor-associated macrophages across a range of tumor-associated macrophage densities (Red: MC38, Green: B16, Blue: KP1.9). The graph shows the percent of anti-PD-1 mAbs bound to macrophages (y-axis; defined as the fraction of $AF647^+$ signal bound to these cells) in tumors with varying percentages of these cells (x-axis; defined as the fraction of $F4/80^+$ $CD11c^+$ cells among $CD45^+$ $7AAD^-$ cells). Linear regression analysis of combined data indicates a non-significant (n.s.) p value for slope deviation from zero. Each datapoint identifies a different tumor.

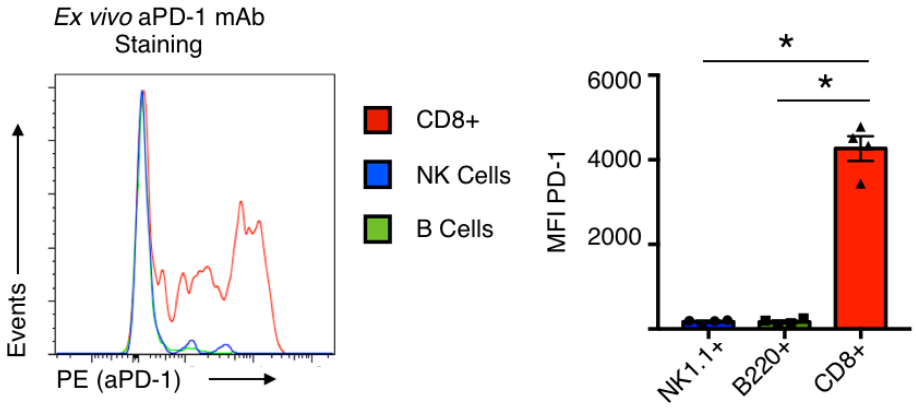

Figure S8: CD8⁺ T cells are the predominant PD-1 expressing cells in the MC38 tumor microenvironment. A representative flow cytometry histogram shows PD-1 expression on CD8+ T cells, NK Cells, and B cells sorted from MC38 tumors implanted intradermally in C57B6 mice. Pooled results from four tumors show substantially higher surface PD-1 expression on tumor infiltrating CD8+ T cells than the negligible levels found on other immune cell types. *$P < 0.05$; two-way ANOVA with Tukey's multiple comparisons test.

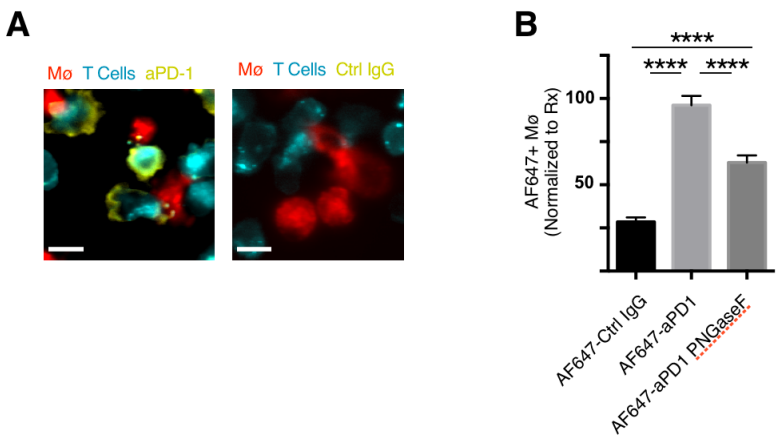

Figure S9. aPD-1 mAb transfer from T cells to macrophages *in vitro*. (A) AF647-aPD-1 (yellow) exchange from T cells (EL-4 cells, in cyan) to macrophages (red) was observed (left) in 3 independent experiments run in parallel with an AF647-labeled control rat IgG2a (right). **(B)** The uptake of AF647+ mAb, quantified relative to the number of AF647-aPD-1 puncta within macrophages, compared with AF647-labeled control rat IgG2a or AF647-labeled PNGaseF-treated aPD-1 mAb. ****$P < 0.0001$; one-way ANOVA. Scale bars represent 10 μm.

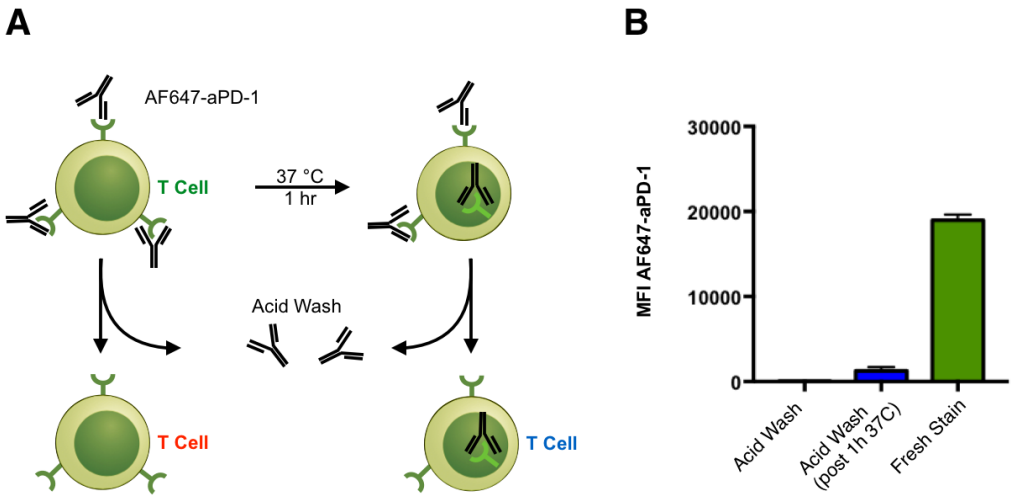

Figure S10: aPD-1 is not internalized following binding to PD-1. (A) An experimental scheme using AF647-aPD-1 stained EL4 lymphocytes incubated at 4 or 37 degrees Celsius provides a model to study antibody internalization. Acid wash removal of surface antibody permits detection of internalized aPD-1 using fluorescence measurements. **(B)** Flow cytometry measurement of AF647-aPD-1 levels in freshly-stained T lymphocytes dropped several orders of magnitude after acid wash removal of surface antibody. Acid stripped lymphocytes incubated at 37 degrees for 1 hour showed negligible levels of internalized AF647-aPD-1. Data represent 2 independent experiments.

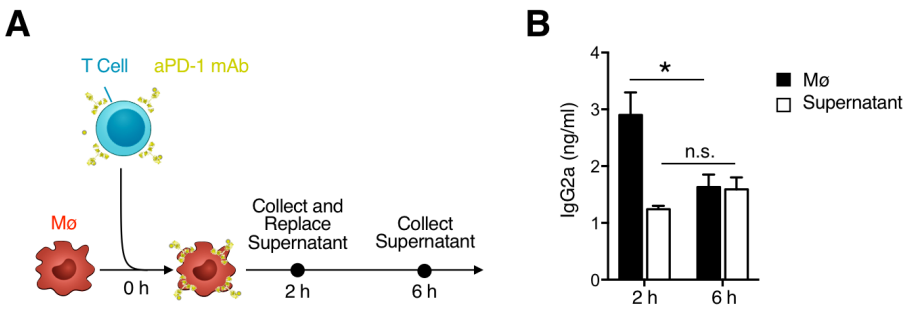

Figure S11: Macrophages degrade aPD-1 mAb after acquisition from T cells. (A) Experimental outline of aPD-1 coated T cell macrophage co-culture conditions. **(B)** ELISA-based detection of rat IgG2a in bone marrow-derived macrophages (Mø) or supernatants after incubation periods (2 and 6 h) following removal of aPD-1-labeled lymphocytes. Antibody detected in macrophages after supernatant replacement was significantly reduced after 4 additional hours of culturing. Antibody release into the supernatant was not detected (n = 3). *$P < 0.05$; t test.

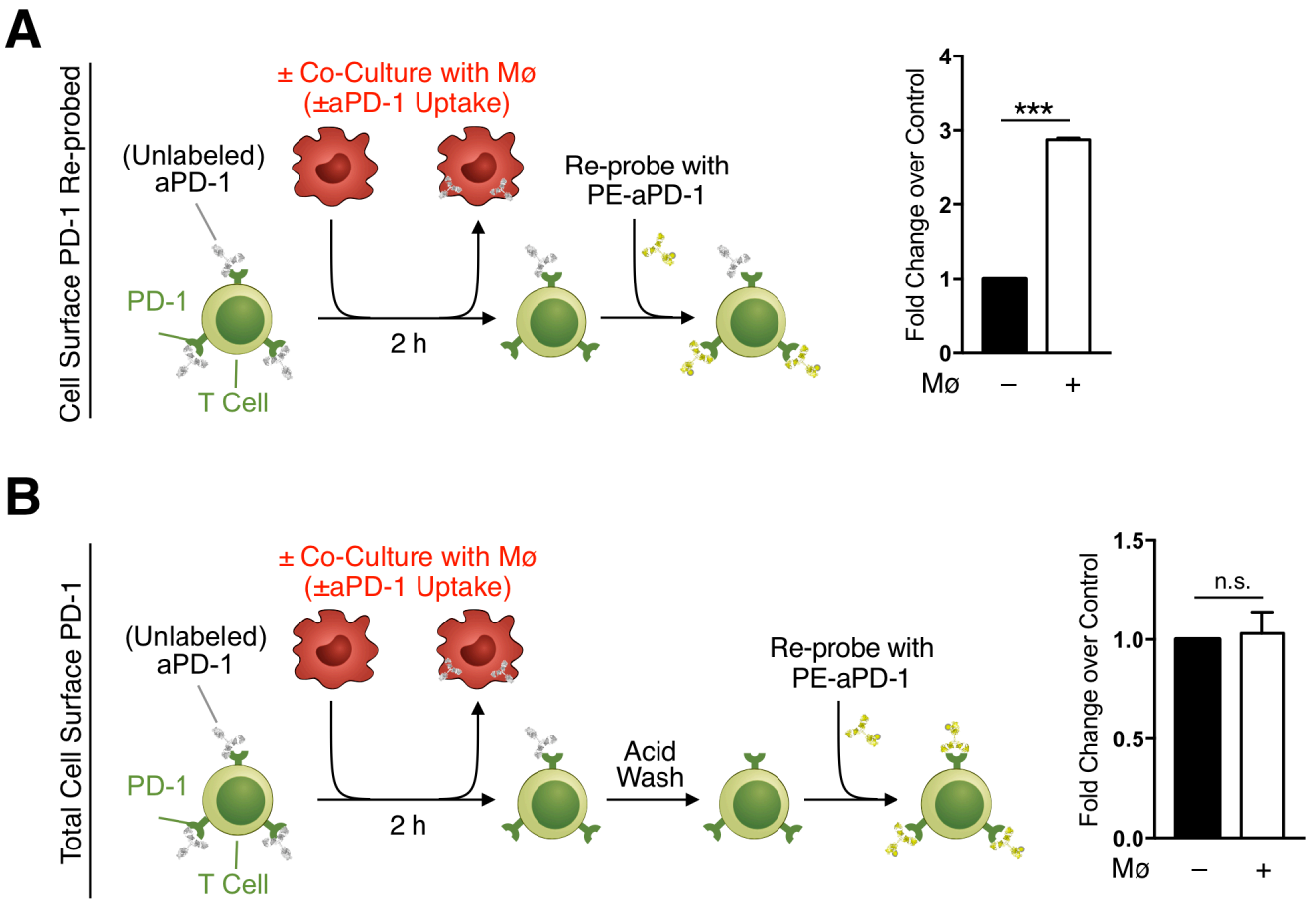

Figure S12: PD-1 remains on the cell surface after the shaving reaction. (A) To determine PD-1 receptor fate after aPD-1 mAb shaving, T cells coated with unlabeled aPD-1 and co-cultured with macrophages (Mø) to permit antibody removal. PD-1 receptor remaining on the T cell surface after antibody shaving is detected by re-staining with PE-aPD-1 after acid washing. Flow cytometric analysis showed Mø removal of aPD-1 permitted binding of PE-aPD-1 to the exposed surface PD-1 on EL4 lymphocytes **(B)**. Following acid wash, PE-aPD-1 levels were high on lymphocytes regardless of Mø exposure, demonstrating PD-1 remains on the lymphocyte surface after antibody shaving. Data represent 2 independent experiments; *$P < 0.05$; **$P < 0.01$; two-way ANOVA with Tukey's multiple comparisons test.

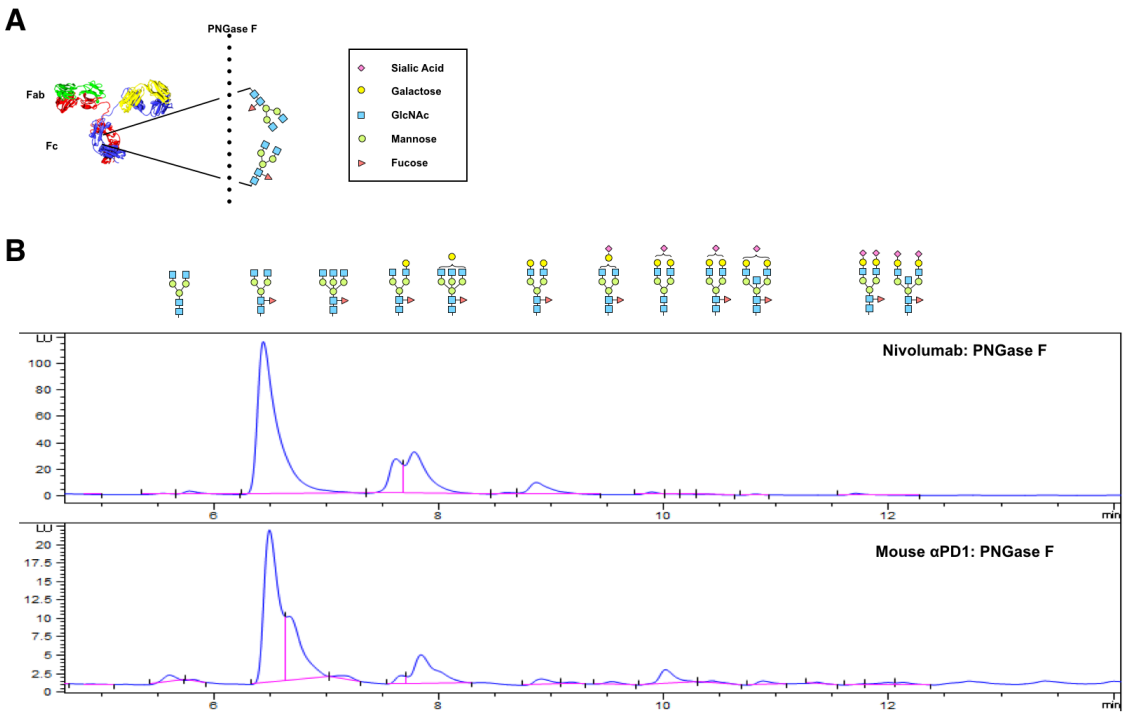

Figure S13. Comparative analysis of mAb glycosylation patterns between mouse aPD-1 and nivolumab. (A) Total glycan was digested from mAb using recombinant PNGase F. **(B)** HPLC analysis of glycan digested from nivolumab (top) or rat IgG2a anti-mouse PD-1 (29F.1A12 clone), and the distribution of glycan structures based on size exclusion. The y-axis is arbitrary units indicative of glycoform abundance, and x-axis is time of elution from the column. The digested glycans from human IVIG were used as a reference to label the elution times for common glycoforms.

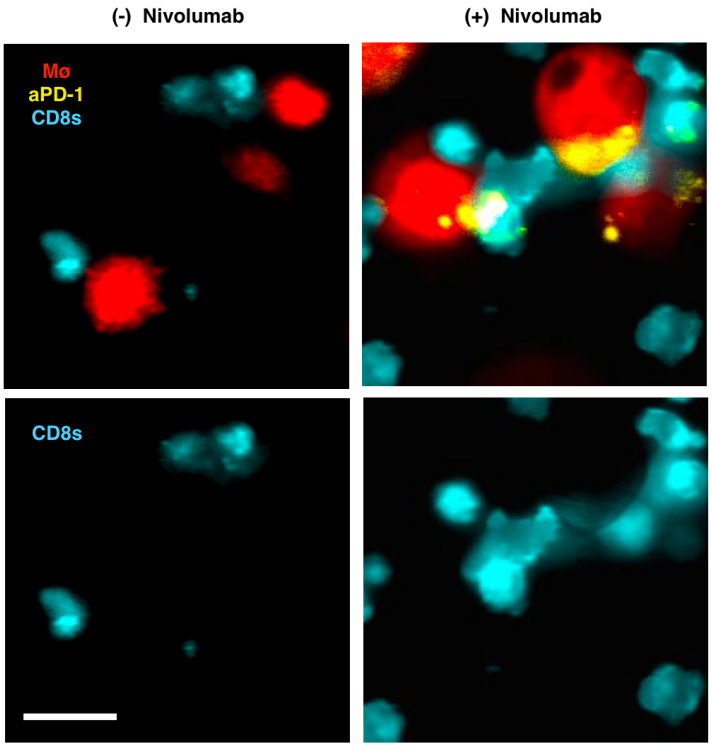

Figure S14: Membrane components are not exchanged after antibody shaving. Time-lapse microscopy of PKH-red labeled human peripheral blood mononuclear cell-derived macrophages co-incubated with aCD3 stimulated PKH-green labeled $CD8^+$ T cells coated with AF647-nivolumab (yellow). Top panels display the merge of PKH-red (macrophages), aPD-1, and PKH-green ($CD8^+$ T cells). Bottom panels display only PKH-green. Images at 30 minutes of co-culture show AF647+ puncta to be devoid of PKH-green membrane dye. Scale bar represents 20 μm.

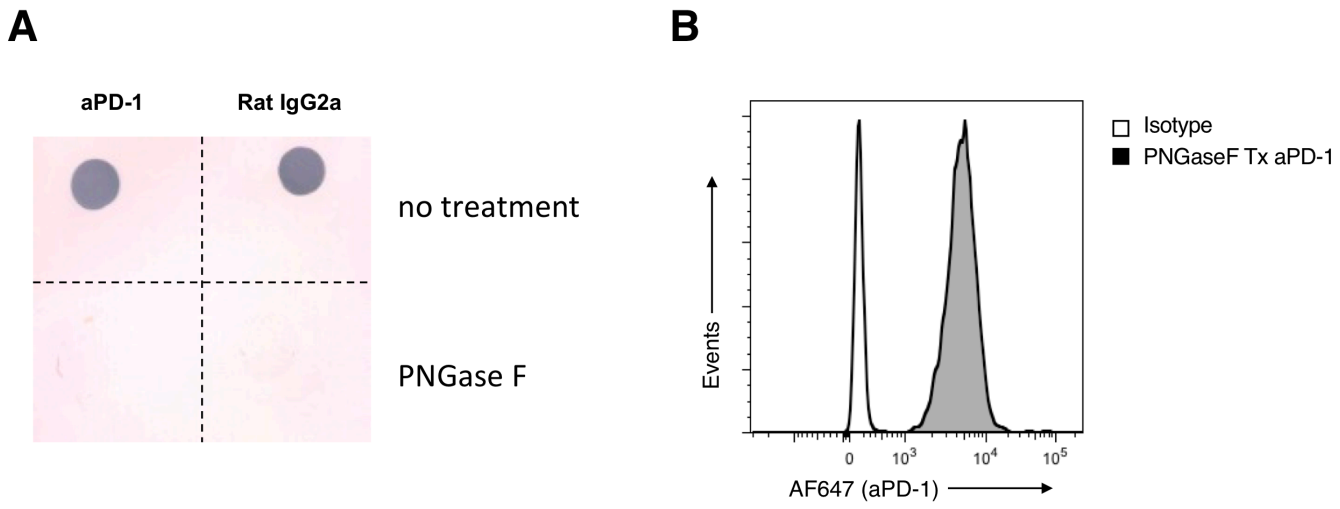

Figure S15. Confirmation of deglycosylation and antigen binding affinity for rat anti-mouse PD-1. (A) Rat anti-mouse PD-1 mAb (clone 29F.1A12) and rat IgG2a isotype control were deglycosylated using PNGase F, and lens culinaris agglutinin (LCA) agent for visualizing sugars was used to confirm complete deglycosylation. **(B)** PNGase F treated aPD-1 conjugated to AF647 and was used to label PD-1 expressing cells (filled histogram). The open histogram is rat IgG2a isotype control staining.

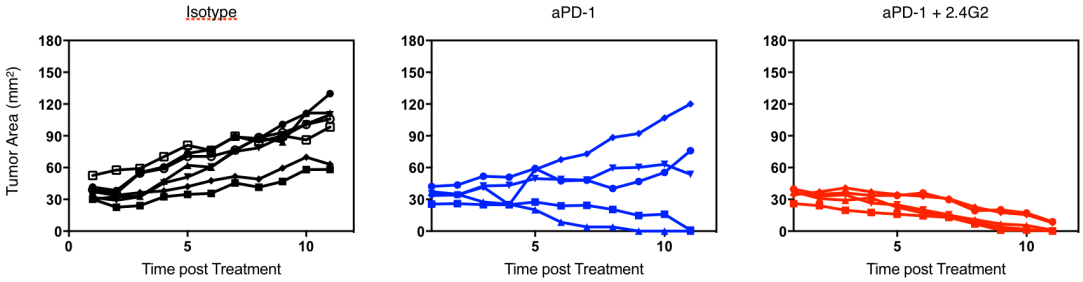

Figure S16: Spider plots of Fc Blocked aPD-1 treatment. MC38 tumor growth curves for individual mice treated with isotype control, aPD-1, or aPD-1 plus 2.4G2 demonstrate the heterogeneity in aPD-1 response and subsequent increase in complete regressions when Fc binding is abrogated.

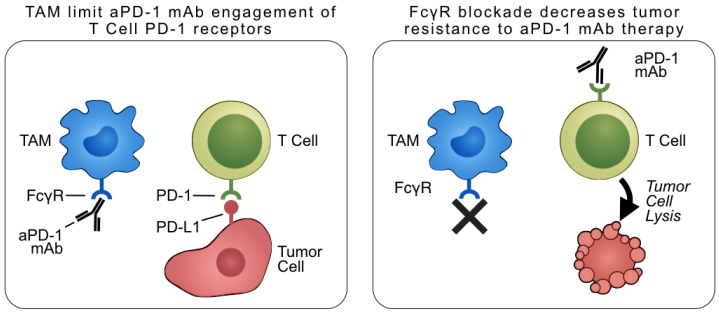

Figure S17: Scheme illustrating that TAM limit aPD-1 mAb engagement on T cells but that inhibiting FcγR can improve aPD-1 mAb therapy. The left panel shows that tumor-associated macrophages (TAM) limit aPD-1 mAb engagement of T cell PD-1 receptors by sequestering the drug using Fcγ receptors (FcγR). PD-1 binding to its ligand (e.g. PD-L1 expressed by tumor cells) inhibits anti-tumor T cell immunity. The right panel shows that FcγR blockade results in aPD-1 retention on T cells. This is turn augments anti-tumor functions and reverses the heterogeneity observed in aPD-1 mAb treatment response.

Supplementary Movies

Movie S1: Intravital microscopy imaging of AF647-aPD-1 injection in a DPE-GFP mouse bearing an MC38-H2B-mApple tumor in a dorsal skin fold chamber. Time-lapse imaging was used to track AF647-aPD-1 distribution. Vasculature and macrophages are labeled with Pacific Blue delivered via dextran or dextran nanoparticle, respectively. Upon i.v. delivery of AF647-aPD-1, drug can be observed in vasculature. Binding to DPE-GFP T cells can be observed as the drug extravasates. These images are projections of Z-stacks with 5 μm thickness.

Color Scheme: White - aPD-1, Red - Tumor cells, Green - T cells, Blue - Macrophages

Movie S2: Intravital microscopy imaging of AF647-aPD-1 injection in an IFNγ-eYFP GREAT mouse bearing an MC38-H2B-mApple tumor in a dorsal skin fold chamber. T cell movement within the tumor microenvironment near a blood vessel (yellow outline) was monitored for 15 minutes prior to i.v. infusion of AF647-aPD-1. Extravasated drug coats T cells and begins forming puncta on the T cell surface after 10 minutes (yellow arrow). One example of aPD-1 mAb transfer from a CD8+ T cell to a PacBlue-ferumoxytol labeled macrophage can be observed at the magenta arrow. Approximately 30 minutes after the mAb first bound T cells, its distribution is largely confined to the neighboring macrophages. These images are projections of Z-stacks with 5 μm thickness.

Color Scheme: White - aPD-1, Red - Tumor cells, Green - T cells, Blue - Macrophages

Movie S3: **Live imaging of mouse T cell aPD-1 transfer to macrophages**. PKH-green labeled T cells (cyan) stained with AF647-aPD-1 (yellow) were co-incubated with murine bone marrow-derived macrophages labeled with PKH-red dye. Videos were acquired in an integrated motarized inverted microscope set-up housed in a climate-controlled environment. Time-lapse images (5 minutes per frame) demonstrate the transfer of AF647-aPD-1 from lymphocytes to macrophages.

Color Scheme: Red - Macrophages, Cyan - T cells, Yellow - aPD-1

Movie S4: Live imaging of human T cell aPD-1 transfer to macrophages Transfer of AF647-nivolumab (yellow) from PKH-green labeled human $CD8^+$ T cells (cyan) to PKH-red labeled human peripheral blood mononuclear cell derived macrophages can be observed by time-lapse imaging (5 minutes per frame).

Color Scheme: Red - Macrophages, Cyan - T cells, Yellow - aPD-1